Analysis of the Bowing Phenomenon for Thin c-Si Solar Cells using Partially Processed c-Si Solar Cells

Jong Rok Lim [1], Sihan Kim [2], Hyung-Keun Ahn [2] , Hee-Eun Song [1] and Gi Hwan Kang [1,*

[1] Photovoltaics Laboratory, New and Renewable Energy Institute, Korea Institute of Energy Research, Daejeon 34129, Korea; jongrok@kier.re.kr (J.R.L.); hsong@kier.re.kr (H.-E.S.)
[2] Department of Electrical and Electronics Engineering, Konkuk University, 120 Neungdong, Gwangjin, Seoul 05029, Korea; kimsian75@gmail.com (S.K.); hkahn@konkuk.ac.kr (H.-K.A.)
* Correspondence: ghkang@kier.re.kr; Tel.: +82-42-860-3418

Abstract: The silicon wafers for solar cells on which the paste is deposited experience a bowing phenomenon. The thickness of commonly used c-Si wafers is 180 μm or more. When fabricating c-Si solar cells with this wafer thickness, the bowing value is 3 mm or less and the problem does not occur. However, for the thin c-Si solar cells which are being studied recently, the output reduction due to failure during manufacture and cracking are attributed to bowing. In generally, it is known that the bowing phenomenon arises mainly from the paste applied to the back side electrode of c-Si solar cells and the effects of SiNx (silicon nitride) and the paste on the front side are not considered significant. The bowing phenomenon is caused by a difference in the coefficient of expansion between heterogeneous materials, there is the effect of bowing on the front electrode and ARC. In this paper, a partially processed c-Si solar cell was fabricated and a bowing phenomenon variation according to the wafer thicknesses was confirmed. As a result of the experiment, the measured bow value after the firing process suggests that the paste on the front-side indicates a direction different from that of the back-side paste. The bow value increases when Al paste is deposited on SiNx. The fabricated c-Si solar cell was analyzed on basis of the correlation between the bowing phenomenon of the materials and the c-Si wafer using Stoney's equation, which is capable of analyzing the relationship between bowing and stress. As a result, the bowing phenomenon of the c-Si solar cell estimated through the experiment that the back side electrode is the important element, but also the front electrode and ARC influence the bowing phenomenon when fabricating c-Si solar cells using thin c-Si wafers.

Keywords: thin c-Si solar cells; bowing phenomenon; warpage; partially processed solar cell

1. Introduction

Current solar power generation is shifting to thinner crystalline silicon (c-Si) solar cells for cost reduction purposes [1]. In 2017, the thickness of the wafers was 180 μm, but by 2028 the thickness of the wafer is expected to decrease to 130 μm. [2]. Therefore, research is also being undertaken to make cells thinner than those currently being used commercially. Reduction in the production cost is essential for grid parity and thin c-Si solar cells are important elements in this context. However many problems arise when fabricating PV (photovoltaic) modules using thin c-Si solar wafers. Typically, bowing occurs during the manufacture of c-Si solar cells; when the bowing phenomenon of the c-Si solar cell becomes severe, micro-cracking occurs. When micro-cracking occurs in the c-Si solar cell, the electrical output of the c-Si solar cell decreases due to changes in Rs (series resistance) and Rsh (shunt resistance). In the PV module, a mismatch of the electrical output occurs due to a decrease in the output of the c-Si solar cell, causing a reduction in the overall electrical output and long-term reliability of the PV module [3–5]

Bowing is caused by a difference in the thermal expansion coefficients between the front/rear-side electrode and the c-Si wafer [6,7]. The coefficient of thermal expansion of silicon is $2.6 \times 10^{-6}/\text{K}$, and the coefficients of thermal expansion of the front electrode and the rear electrode are $19.7 \times 10^{-6}/\text{K}$ and $23.9 \times 10^{-6}/\text{K}$, respectively [7]. Therefore, when manufacturing a c-Si solar cell, a bowing phenomenon occurs due to this difference in thermal expansion coefficients. To minimize the occurrence of cracks, it is important to minimize the bowing phenomenon during c-Si solar cell manufacture. In the process of thin c-Si solar cell manufacture, the bowing phenomenon occurs during the firing process and the bowing of thin c-Si solar cells causes micro-cracks and stress leading to problems in the PV modularization process.

Research on bowing in the photovoltaic module has mainly concentrated on the thickness of the PV ribbon and the process temperature during the tabbing step [7–9]. In the process of manufacturing c-Si solar cells, only the influence of the back-side electrode (Al paste) on the bowing phenomenon has been studied. However, studies on the influence of the anti-reflection coating (ARC) and front-side electrode on the bowing phenomenon have not progressed [10–17]. In order to accurately analyze the bowing phenomenon of solar cells, it is important to measure the bowing of the c-Si solar cell by manufacturing a partially processed c-Si solar cell. Also, if the thickness of the c-Si wafer is thick, it may be difficult to accurately identify the bowing phenomenon. Therefore, it is necessary to analyze the bowing phenomenon using a thin c-Si solar cell.

In this paper, we fabricated solar cells using c-Si solar wafers with thicknesses of 120, 140, 160, and 180 μm. The bowing value was then measured after the firing process, and the bowing phenomena of the wafer, ARC, and front/back-side electrode were analyzed. Through the experimental results, it was confirmed that the bowing phenomenon of the c-Si solar cell is influenced not only by the back side electrode, but also by the front side electrode and silicon nitride (SiNx).

Based on the experimental results, intrinsic stress values were calculated using Stoney's Equation and the main factors of the bowing phenomenon in the manufacturing process of c-Si solar cells using c-Si wafers were analyzed.

2. Bowing Phenomenon of c-Si Solar cells

2.1. Bowing characteristics of thin c-Si solar cells

Generally, a c-Si solar cell is fabricated as shown in Figure 1. Starting with a c-Si solar wafer substrate, after texturing, doping, and etching processes, and by depositing an ARC, it is possible to produce a c-Si solar cell with a dry and firing process on the front electrode and back electrode.
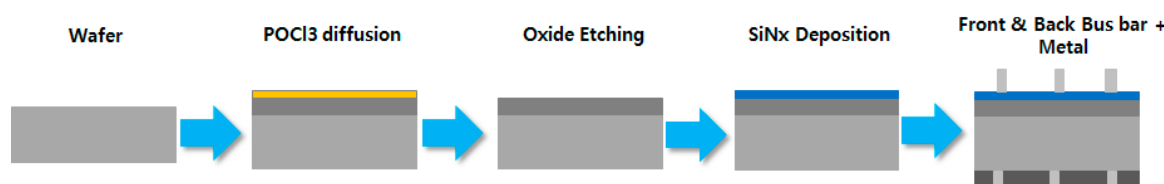
Figure 1. c-Si Solar cell manufacturing process.

The process for fabricating the c-Si solar cell includes a variety of thermal stress environments such as doping, etching, and chemical vapor deposition. This thermal stress can damage the c-Si wafer and the paste; when the thickness of the wafer is greater than 180 μm, cracking due to thermal stress is rare. However, as the thickness is reduced, micro-cracks are generated by thermal stress between the different materials. c-Si solar cell bowing depending on the coefficient of thermal expansion (CTE) between materials is more pronounced after the firing process.

In the drying process, the surface temperature of the c-Si wafer was measured using data log, as shown in Figure 2. Substantial bowing did not occur below 200 °C. However, in the firing process

for depositing the c-Si wafer and metal (ARC, front/back-side electrode), a temperature of about 800 °C or higher was measured; after this process, serious bowing could be confirmed, as shown in Figure 3.

Figure 2. Temperature measurement using data log in drying and firing processes.
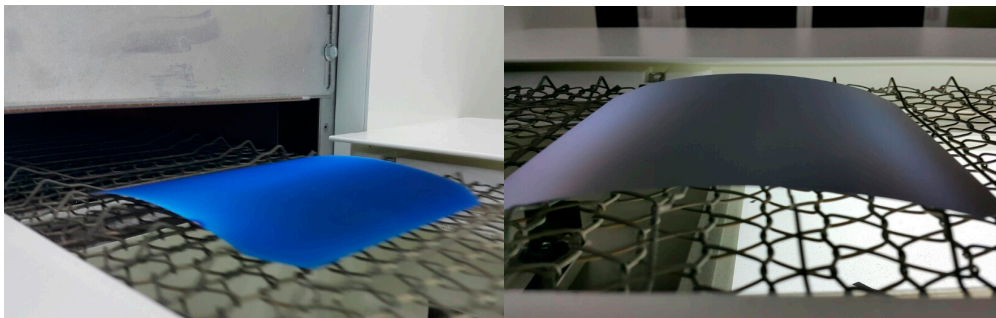
Figure 3. Bowing phenomenon after firing process of c-Si solar cell which is partially processed.

2.2. Theoretical analysis of bowing phenomenon of c-Si solar cells

The bowing of the c-Si solar cells is caused by the c-Si wafer, front/back electrodes, and ARC. The stress of the film is represented by σ_f and the whole stress is expressed by the intrinsic stress (σ_i) and thermo-mechanical stress (σ_{th}) as in Equation (1) [18–21]:

$$\sigma_f = \sigma_i + \sigma_{th} \tag{1}$$

Expressions of stress can be predicted by Stoney's equality [21]. Stress is the relationship between Young's modulus and strain, and the curvature of the heterogeneous material assuming pure bending and small bending can be expressed using Stoney's equation:

$$\frac{1}{R} = \frac{6E_f t_f \left(\alpha_f - \alpha_s \right) \left(T_f - T \right)}{E_s t_s^2} \tag{2}$$

where t_s and t_f are the substrate thickness and thickness of the film, respectively. E_f, E_s are the Young's moduli of the film and substrate. α_f is coefficient of expansion of the film and T_f is the temperature of substrate, T is room temperature.

Mechanical analysis of Stoney's equation assumes that the length of the substrate and film are the same. c-Si solar cells have the same length of material deposited on the c-Si wafers, so Stoney's equation assumptions are expected to fit well. Also, Stoney's equation cannot be applied when the process temperature is different, but the temperature of the deposition process is identical during the c-Si solar cell manufacturing process so this assumption is fulfilled.

Stoney's equation is applied to c-Si solar cells assuming bending of the beam and small bending. It follows that:

$$E_s \frac{4t_s^2}{3t_f L^2} = E_f \left(\alpha_f - \alpha_s \right) \left(T_f - T \right) \tag{3}$$

This is a basic condition in the assumption of small bending. It is possible to assume small bending and calculate this expression with a Taylor expansion [21]. Here, L is the length of the c-Si wafer. In other words, the bowing value can be calculated from the stress value of the film, and the stress value of materials can be calculated by measuring the bowing value. Using Equation (3), the stress values of ARC and the front/back electrodes of the c-Si solar cells can be deduced. In this paper, using the bowing value that is measured through the experiment, the stress values of ARC and electrode of the c-Si solar cell were confirmed.

3. Experiment Methods and Conditions

3.1. Experimental Conditions

To confirm the bowing phenomenon dependence on the thickness of the c-Si wafer, a high-efficiency single c-Si wafer was prepared. When wafer thickness deviation occurs, errors occur. For this reason, to confirm the bowing phenomenon, wafer sorting was carried out using appropriate wafer inspection equipment prior to the experiment.

The c-Si wafers were prepared with thicknesses ranging from 120 μm to 180 μm in 20 μm intervals. For the 120 μm wafer, samples were prepared with an error range of approximately 1.7% between the wafer to wafer thickness variation. Further, the 180 μm wafers in the experiment had an average thickness of 183.1–183.5 μm and the 140 and 160 μm wafers also exhibited an error range of 2% using the same method. After the firing process, the bowing was measured using a Vernier caliper divided in 1 mm after placing the c-Si solar cells on a flat surface. As the bowing value decreases over time, the temperature was measured immediately after the fitting process. At this time, the temperature was 25 °C.

The surface of the wafer after the diamond sawing process, which is one of the wafer manufacturing steps, is shown in Figure 4. When the strength was applied in the same direction as the sawing mark of c-Si wafer, the strength was weaker than in the horizontal direction. Therefore, c-Si solar cells were manufactured in the same direction in consideration of this.
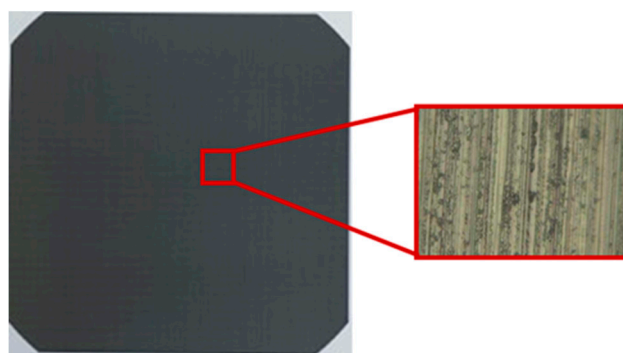
Figure 4. Wafer surface measured using an optical microscope.

To confirm the influence of the electrode deposited on the wafer, solar cells in which the process was partially performed were prepared. The bowing phenomenon occurs due to the differences in coefficient of thermal expansion (CTE) between different materials and does not occur on the bare wafer. In other words, as shown in Figure 5, bowing phenomena does not occur in bare wafers, or during the texturing, etching, and doping processes.

```
┌─────────────────────────────────┐
│  Saw damage Removal & Cleaning  │
└─────────────────────────────────┘
                 ↓
┌─────────────────────────────────┐
│    Both side pyramid Texturing  │
└─────────────────────────────────┘
                 ↓
┌─────────────────────────────────┐
│      Pocl₃ Doping Process       │
└─────────────────────────────────┘
                 ↓
┌─────────────────────────────────┐
│         Oxide cleaning          │
└─────────────────────────────────┘
                 ↓
┌─────────────────────────────────┐
│      Front SiNx deposition      │
└─────────────────────────────────┘
                 ↓
┌─────────────────────────────────┐
│      Screen Printing & Drying   │
└─────────────────────────────────┘
                 ↓
┌─────────────────────────────────┐
│      Co-Firing Metallization    │
└─────────────────────────────────┘
                 ↓
┌─────────────────────────────────┐
│           Measurement           │
└─────────────────────────────────┘
```

Figure 5. Solar cell fabrication sequence.

3.2. Partial Solar Cell Fabrication Process According to the c-Si Wafer Thickness

Partially processed solar cells were fabricated as shown in Table 1 using a 6 inch single c-Si wafer. Since the bowing phenomenon does not occur after the firing process in the case of the c-Si wafer that only undergoes the etching and the doping processes, bowing is hardly displayed in the process of depositing SiNx on the c-Si wafer. Thus it was excluded from the design of experiments (DOE) listed in Table 1.

Table 1. Design of experiments (DOE) of partially processed solar cells according to the thickness of the c-Si wafer. ARC: anti-reflection coating.

c-Si Wafer Thickness	Num	ARC	Front Side Electrode	Back Side Electrode
	1	o	o	o
	2	x	o	o
120 μm, 140 μm, 160 μm, 180 μm	3	o	o	x
	4	x	o	x
	5	o	x	o
	6	x	x	o

Solar cells were fabricated with the Gumi Electronics & Information Technology Research Institute (GERI) and experiments were performed under the same conditions (except for the wafer thickness) to minimize errors. In Table 1, "Num" is the experiment number and "ARC" refers to the antireflection coating. The front-side electrode indicates Ag paste printing on the wafer's front side, and the back-side electrode, the Al paste.

4. Results and Analysis

To study the bowing phenomenon in the manufacture of solar cells, the wafer and several elements were analyzed to determine the causes of bowing. Our previous research dealt with the study of the back-side electrode. SiNx (ARC) has a large intrinsic stress value, but its thickness is about 80 nm and so it is hardly affected when it is deposited on a thick wafer of 180 μm or more. As expected, in the case of the front-side electrode, bowing was hardly observed experimentally for 180 μm wafer thickness or more.

Experiments 4 and 6, shown in Figure 6, represent the deposition of the front-side paste and back-side paste on the Si wafer. In this experiment, 10 c-Si wafer pieces were measured, and values

below 1 mm were excluded from the measurements. The Experiment 4 results indicate that the bow value increases unconventionally as the wafer thickness decreases. However, in Experiment 6, the bow form is concave facing down, and that of Experiment 4 is concave facing up. In other words, the bowing is caused by differences between the front-side paste and back-side paste. Figure 7 is a comparison of bowing values of general solar cells and solar cells excluding ARC.
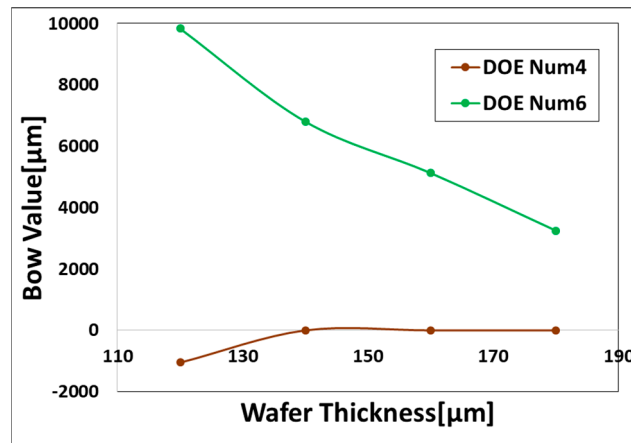
Figure 6. Results of bow experiments 4 and 6.
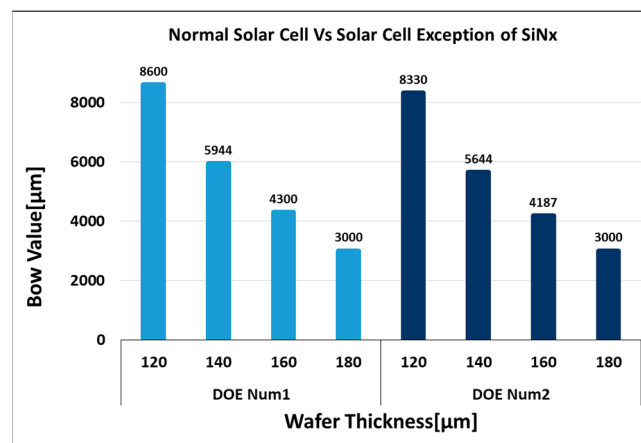
Figure 7. Bowing phenomenon due to thickness of wafer and presence or absence of ARC (anti-reflection coating) deposition on a c-Si wafer.

Figure 7 shows the bowing experiment results with and without ARC in a general solar cell. There is no difference in bowing when the thickness of the wafer is 180 μm. It is confirmed that as the wafer becomes thinner a difference occurs in the bowing value. In other words, in the case of a solar cell fabricated using a wafer of 180 μm or more, it is impossible to ascertain the difference in bowing value due to the ARC, but it is confirmed that as the thickness of the wafer reduces, a difference occurs in the bowing phenomenon. The reason is that the bowing value increases as the thickness of the c-Si wafer becomes thinner. When only the ARC of the wafer is deposited, it is difficult to confirm because the value of the bowing is too small. However, when the back electrode is printed, the difference of the bowing value can be confirmed.

Figure 8 shows a bowing experiment result with and without Ag paste, which is the front-side electrode. When only the front-side electrode is deposited on the silicon wafer, bowing hardly occurs unless the thickness of the wafer is 120 μm. The influence of the front-side electrode paste on the bowing according to the thickness of the wafer is difficult to ascertain. However, as shown in Figure 8, when there is a back electrode on the c-Si wafer, it is possible to confirm the influence of the front-side electrode on the bowing phenomenon of the solar cell.
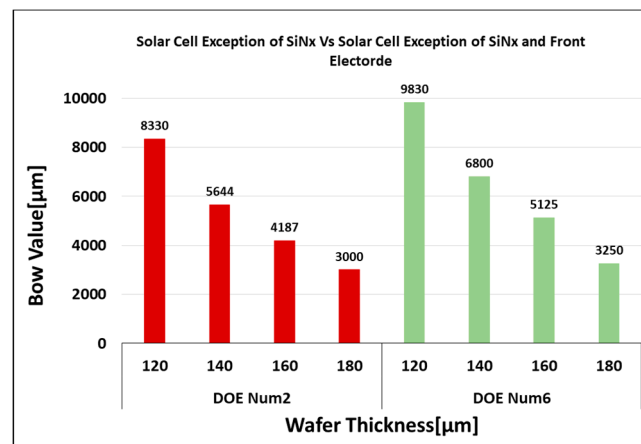
Figure 8. Bowing phenomenon due to thickness of wafer and presence or absence of front-side electrode deposition on a c-Si wafer.

DOE Num2 means that the front-side electrode and the back-side electrode were deposited on the wafer and DOE Num 6 refers to the case where only the back-side electrode was deposited. When the thickness of the wafer is 180 μm, the difference in bowing value is about 0.5 mm. The difference in bowing size is small, but when the wafer thickness is 120 μm, a difference of 1.5 mm in the bowing value is confirmed, so as the wafer becomes thinner, and when the thickness of the wafer is 120 μm, the difference in the bowing value increases by about 1.0 mm.

DOE Num3 in Figure 9 reveals that in the absence of the back-side electrode, the bowing phenomenon is negligible when the thickness of the wafer is 140 μm or more, and the bowing direction is reversed in the case of only the front paste and the ARC.
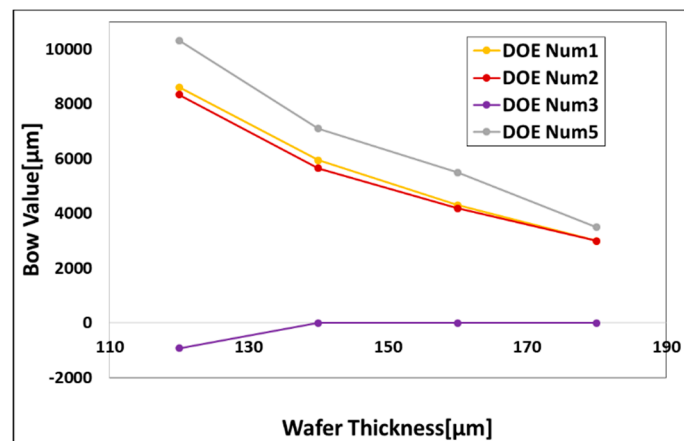
Figure 9. Results of bow experiments 1, 2, 3, and 5.

In addition, when comparing DOE Num1 (an ordinary solar cell) with DOE Num5 (in which the front-side electrode is not deposited on the c-Si wafer), it can be confirmed that the bowing value increases in the absence of the front electrode. Experiment 3 is a bowing value measured after deposition of only the front-side electrode on the c-Si wafer, and it can be confirmed that the bowing direction differs from that of the other materials.

To estimate the stress value through the bowing value, it is important to know the exact thickness of the c-Si wafer and each material. The thickness of each material can be measured through scanning electron microscopy (SEM) and the result is shown in Figure 10. It is important to know the thickness of the c-Si wafer and each material. After cutting the solar cell, the side was measured and the thickness of each material measured in SEM was assumed to be a constant value in a c-Si solar cell. The wafer

thickness of the solar cell of Figure 10 is thinner than that of the bare wafer, due to the chemical etching step during the solar cell manufacturing process.
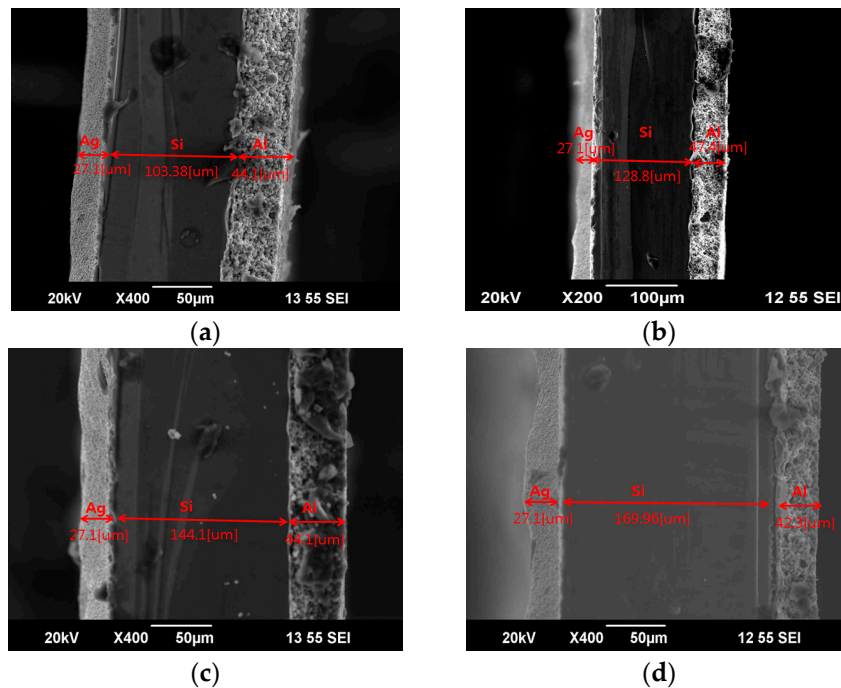
Figure 10. SEM measurement result according to wafer thickness. (**a**) SEM measurement result of 120 μm c-Si solar cell; (**b**) SEM measurement result of 140 μm c-Si solar cell; (**c**) SEM measurement result of 160 μm c-Si solar cell; (**d**) SEM measurement result of 180 μm c-Si solar cell.

Through the bowing experiment results, the stress value generated in the processing of the solar cell was predicted. The bow phenomenon of a bi-material can be analyzed using Stoney's equation. According to the equation, stress values can be predicted through the measured bow value; on the other hand, knowing the stress value of the material in the deposition process can predict the bowing value. In this paper, partially processed solar cells were fabricated with varying thickness, and the stress value was predicted from the bowing value of each material measured.

In a previous study, we analyzed the intrinsic stress of the front ARC of a solar cell [22]. Experiment results showed the bowing value due to ARC deposition on the wafer as small, when the thickness of ARC is very thin (about 80 nm). As a result, the stress value was expected to be very large at 253 MPa. To conclude, it is expected that the influence of bowing by ARC will be large when the thickness of ARC increases or the c-Si wafer becomes thinner. That is, it can be confirmed that the value of bowing is 1 mm or less and substantial bowing occurs although it is small.

Figure 11 shows the result of predicting the intrinsic stress value of ARC and c-Si wafer using Stoney's equation. Although the magnitude of the bowing value by ARC is small, one can confirm that the bowing value exists.
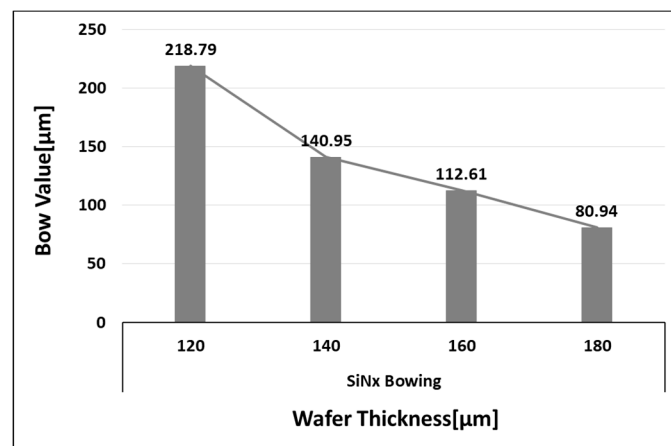
Figure 11. Influence of ARC on bowing phenomenon according to the thickness of c-Si wafers.

Through experiments, the bow value depending on the presence or absence of the front electrode was confirmed. However, when the front-side electrode is deposited on the wafer, if the thickness of the wafer is 140 μm or more, the experimental bow value result is 1 mm or less and its value is not displayed. The front electrode has a small intrinsic stress value and has smaller influence on the bow phenomenon due to its lower thickness than the back electrode. The bowing value varies when the front side electrodes are present in DOE 1 and 5 in Figure 9. The results of Experiment 4, which deposited only the front electrodes in the c-Si wafer, were measured only when the wafer was 120 μm thickness. This is because it is difficult to measure a bowing value if it is less than 1 mm. That is, bowing occurs even on a wafer that is than 140 μm or more of thickness. Figure 12 shows the estimated intrinsic stress values from the front electrode and 120 um c-Si wafer deposition and the result is calculated using Stoney's equation. In the case of the front electrode, it could be predicted from the results that bowing occurs in a direction different from that of the ARC and the back-side electrode. In the case of the front electrode, it appears as a phenomenon that reduces the bowing value of the solar cell.
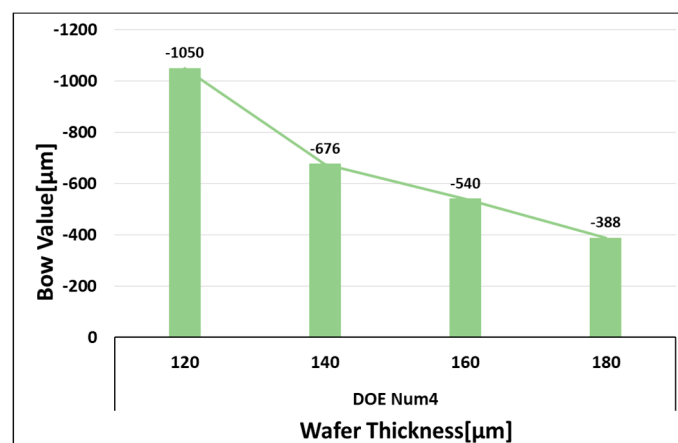
Figure 12. Influence of the front-side electrode on bow phenomenon according to thickness of c-Si wafers.

Through the experimental results, it was confirmed that the deposition of the back-side electrode greatly affects the bowing of the c-Si solar cell. The stress value of the back electrode calculated using Equation (3) is about 20 MPa and its value is as small as about 10% when compared with the intrinsic stress of SiNx. However, the thickness of the back-side electrode is larger than that of SiNx and this greatly affects the bowing phenomenon of the solar cell.

That the back-side electrode has a big influence on the bowing phenomenon is not a material property but rather is largely influenced by the thickness. This means that the thickness of the back-side electrode becomes an important factor in the reduction of bowing. Figure 13 shows the intrinsic stress values predicted using Equation (3) and the bowing values confirmed through experiments.
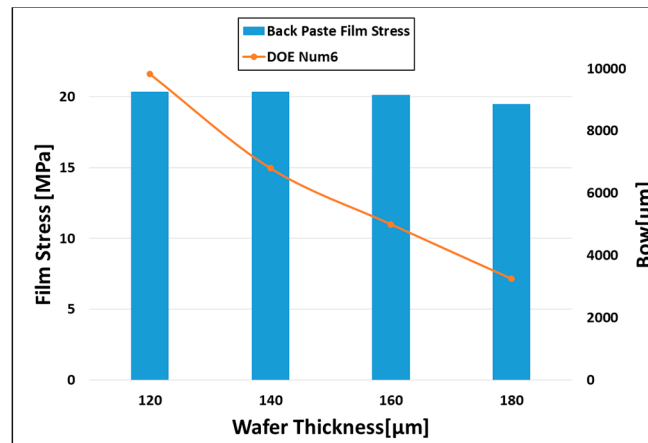
Figure 13. The bowing value and stress value of the back electrode according to change in thickness of the wafer.

5. Conclusions

We studied the bowing phenomenon due to the deposition of the front/back-side electrode and the ARC in accordance with the change in wafer thickness. It is known that the bowing phenomenon of solar cells occurs only on the back-side electrode. In fact, when fabricating a solar cell using a wafer of more than 180 μm thickness, the influence of bowing was very small, except for the back-side electrode. However, as the thickness of the c-Si wafer reduces, as shown in the experimental results, it can be seen that the bowing value varies depending on the ARC and the front-side electrode. Therefore, we were able to confirm their effect on the solar cell bow phenomenon.

In this paper, partially processed c-Si solar cells with different wafer thicknesses were fabricated to analyze the bowing phenomenon of c-Si solar cells. As an experiment result of our study of the bowing phenomenon of partially processed c-Si solar cells using thin c-Si solar cells, in the case of the front electrode, bowing phenomena occurred in different directions from the back side electrode. In addition, when ARC was deposited on a c-Si solar cell, the bowing phenomenon could not be confirmed when the thickness of the wafer was 180 μm or more, but the bowing phenomenon could be confirmed when the thickness of the c-Si wafer was thin.

Also, using Stoney's equation, which can analyze bowing and stress between different materials, it is possible to infer the intrinsic stress value through the bowing value using experimental results. In the previous study, ARC confirmed the stress value using Acro Metrix AXP, and in the case of the front electrode the value of the intrinsic stress cannot be known since the change in bowing is not large when the thickness of the wafer is 140 μm or more. However, we confirmed the value of the intrinsic stress using the bowing value at a wafer thickness of 120 μm. The back-side electrode effect is confirmed as shown in Figure 13 and finally the ARC and front-side electrode have bow values too, but the most important factor was found to be the back-side electrode. By confirming the value of the intrinsic stress for each element of the solar cell, it is expected that this result can be utilized to reduce the bowing phenomena of thin c-Si solar cells.

Author Contributions: J.R.L. wrote the main part of the paper, in particular, the research direction of the paper and the analysis of the experiment. G.H.K. reviewed and revised the overall contents of the paper. S.K. analyzed the data using the paper and provided important comments. H.-K.A established the research direction of the paper and suggested a method for conducting the experiment. H.-E.S provided technical ideas and assistance in establishing the experiment.

Conflicts of Interest: The authors declare no conflicts of interest.

References

1. Demant, M.; Rein, S.; Krisch, J.; Schoenfelder, S.; Fischer, C.; Bartsch, S.; Preu, R. Detection and analysis of micro-cracks in multi crystalline silicon wafers during solar cell production. In Proceedings of the 2011 37th IEEE Photovoltaic Specialists Conference, Seattle, WA, USA, 19–24 June 2011; pp. 1641–1646.
2. Metz, A.; Fischer, M.; Trube, J. International Technology Roadmap for Photovoltaic 2018, 8th ed.; 2017. Available online: http://www.etip-pv.eu/fileadmin/Documents/ETIP_PV_Conference_2017_Presentations/Session_II._1._Axel_Metz.pdf (accessed on 23 April 2019).
3. Pietzer, T.M.; van Molken, J.I.; Ribland, S.; Breitenstein, O. Influence of cracks on the local current–voltage parameters of silicon solar cells. *Prog. Photovolt.* **2015**, *23*, 428–436. [CrossRef]
4. Meyer, E.L.; van Dyk, E.E. Assessing the Reliability and Degradation of Photovoltaic Module Performance Parameters. *IEEE Trans. Reliab.* **2004**, *53*, 83–92. [CrossRef]
5. Kaushika, N.D.; Rai, A.K. An investigation of mismatch losses in solar photovoltaic cell networks. *Energy* **2007**, *32*, 755–759. [CrossRef]
6. Chen, C.H.; Lin, F.M.; Hu, H.T.; Yeh, F.Y. Residual stress and bow analysis for silicon solar cell Induced by soldering. In Proceedings of the International Symposium on Solar Cell Technologies, Taipei, Taiwan, 4–6 December 2008. Available online: http://140.116.36.16/paper/c37.pdf (accessed on 23 April 2019).
7. Lai, C.M.; Su, C.H.; Lin, K.M. Analysis of the thermal stress and warpage induced by soldering in monocrystalline silicon cells bowing. *Appl. Therm. Eng.* **2013**, *55*, 7–16. [CrossRef]
8. van Amstel, T.; Popovich, V.; Bennett, I.J. A Multiscale model of the Aluminium Layer at The Rear side of a Solar cell. In Proceedings of the 24th European Photovoltaic Solar Energy Conference and Exhibition, Hamburg, Germany, 21–25 September 2009.
9. Yoon, P.; Joo, K.; Baek, T.; Song, H.; Chung, H.S.; Shin, S. Measurement of Bow in Silicon Solar Cell Using 3D Image Scanner. *Korean Soc. Mech. Eng.* **2012**, *11*, 1738–1739.
10. Tae-Hyeon, B.; Ji-Hwa, H.; Kee-Joe, L.; Gi-Hwan, K.; Min-Gu, K.; Hee-Eun, S. Bow reduction in thin crystalline silicon solar cell with control of rear aluminum layer thickness. *J. Korean Sol. Energy Soc.* **2012**, *32*, 194–198.
11. Mader, C.; Eitner, U.; Kajari-Schröder, S.; Brendel, R. Bow of Silicon Wafers After In-Line High-Rate evaporation of Aluminum. *IEEE J. Photovolt.* **2013**, *3*, 212–216. [CrossRef]
12. Hilali, M.M.; Gee, J.M.; Hacke, P. Bow in screen printed back contact industrial silicon solar cells. *Sol. Energy Mater. Sol. Cells* **2007**, *91*, 1228–1233. [CrossRef]
13. Kim, S.; Sridharan, S.; Khaditkar, C.; Shaikh, A. Aluminum pastes(lead-free/flow-bow) for Thin Wafers. In Proceedings of the Conference Record of the Thirty-first IEEE Photovoltaic Specialists Conference, Lake Buena Vista, FL, USA, 3–7 January 2005; pp. 1100–1102.
14. Coulter, W.H.; Czyzewicz, R.C.; Farneth, W.E.; Prince, A.; Rajendran, R.G. Using Finite Element Methods and 3D Image Correlation to Model Solar Cell Bowing. In Proceedings of the Photovoltaic Specialists Conference (PVSC), Philadelphia, PA, USA, 7–12 June 2009; pp. 160–267.
15. Bähr, M.; Dauwe, S.; Lawerenz, A.; Mittelstädt, L. Comparison of bow-avoiding Al-pastes for thin, large-area crystalline silicon solar cells. In Proceedings of the 20th Photovoltaic Solar Energy Conference, Barcelona, Spain, 6–10 June 2005.
16. Schneider, A.; Gerhards, C.; Fath, P.; Bucher, E. Bow Reducing Factors for Thin Screen Printed Mc-Si Solar cells with Al BSF. In Proceedings of the Conference Record of the Twenty-Ninth IEEE Photovoltaic Specialists Conference, New Orleans, LA, USA, 19–24 May 2002; pp. 336–339.
17. Frank, H. Aluminum-back surface field: Bow investigation and elimination. In Proceedings of the 20th European Photovoltaic Solar Energy Conference and Exhibition, Barcelona, Spain, 6–10 June 2005.
18. van Silfhout, R.B.R.; van Driel, W.D.; Liz, Y.; Zhang, G.Q.; Emst, L.J. Prediction of Back-End Process induced wafer warpage and Experimental Verifican. In Proceedings of the Electronic Components and Technology Conference, San Diego, CA, USA, 28–31 May 2002; pp. 1182–1187.

19. Lim, J.; Ham, S.; Jeong, B. Warpage modeling and characterization to simulate the fabrication process of wafer-level adhesive bonding. In Proceedings of the Electronic Manufacturing Technology Symposium, San Jose, CA, USA, 3–5 October 2007.

20. Schwarzer, N.; Richter, F. On the determination of film stress from substrate bending: STONEY´s formula and its limits. 2006. Available online: https://monarch.qucosa.de/api/qucosa%3A18453/attachment/ATT-0/ (accessed on 23 April 2019).

21. Gerald, S.G. The tension of metallic films deposited by electrolysis. *Proc. R. Soc. A* **1909**, *82*, 172–175.

22. Kim, S.; Lim, J.; Min, Y.; Ahn, H. Warpage behavior of thin solder cell package. In Proceedings of the 22nd Korean Confernce on Semiconductors (KCS), Incheon, Korea, 10–12 February 2015; p. 58.